Translational Oncology
www.transonc.com

Volume 13 Number 2 Month xxxx pp. 481–489 481

Targeting the IκB Kinase Enhancer and Its Feedback Circuit in Pancreatic Cancer☆

Sridevi Challa[*], Kazim Husain[†], Richard Kim[†], Domenico Coppola[‡], Surinder K. Batra[§], Jin Q. Cheng[*] and Mokenge P. Malafa[†]

[*]Departments of Molecular Oncology, Tampa, FL, USA; [†]Gastrointestinal Oncology, Tampa, FL, USA; [‡]Pathology, H. Lee Moffitt Cancer Center and Research Institute, Tampa, FL, USA; [§]Department of Biochemistry and Molecular Biology, College of Medicine, University of Nebraska Medical Center, Omaha, NE, USA

Abstract

Pancreatic ductal adenocarcinoma (PDAC) is a deadly disease with an overall median 5-year survival rate of 8%. This poor prognosis is because of the development of resistance to chemotherapy and radiation therapy and lack of effective targeted therapies. IκB kinase enhancer (IKBKE) overexpression was previously implicated in chemoresistance. Because IKBKE is frequently elevated in PDAC and IKBKE inhibitors are currently in clinical trials, we evaluated IKBKE as a therapeutic target in this disease. Depletion of IKBKE was found to significantly reduce PDAC cell survival, growth, cancer stem cell renewal, and cell migration and invasion. Notably, IKBKE inhibitor CYT387 and IKBKE knockdown dramatically activated the MAPK pathway. Phospho-RTK array analyses showed that IKBKE inhibition leads to rapid upregulation of ErbB3 and IGF-1R expression, which results in MAPK-ERK pathway activation—thereby limiting the efficacy of IKBKE inhibitors. Furthermore, IKBKE inhibition leads to stabilization of FOXO3a, which is required for RTK upregulation on IKBKE inhibition. Finally, we demonstrated that the IKBKE inhibitors synergize with the MEK inhibitor trametinib to significantly induce cell death and inhibit tumor growth and liver metastasis in an orthotopic PDAC mouse model.

Translational Oncology (2020) 13, 481–489

Introduction

Pancreatic ductal adenocarcinoma (PDAC) is one of the most aggressive cancers and is projected to be the second leading cause of cancer mortality in the United States by 2030, accounting for 63 000 deaths per year [1,2]. The main mutation in 95% of PDAC patients is *KRAS*; however, direct targeting of mutant KRAS has been challenging [3]. Therefore, strategies to target downstream signals of KRAS are currently under investigation.

Current treatment strategies for pancreatic cancer include surgery, chemotherapy, and chemoradiation therapies. Patients who become resistant to these treatments present with highly lethal metastatic tumors. Cancer stem cells (CSCs) with self-renewing capacity have been identified in PDAC. In addition to tumor initiation, these pancreatic CSCs have been implicated in chemoresistance and cancer metastasis [4] Therefore, identification of molecules that are both downstream of *KRAS* and can control pancreatic CSCs may lead to new treatment strategies for this malignancy.

IκB kinase enhancer (IKBKE) has been identified as an important oncogene in several cancers [5–8]. Overexpression of IKBKE may result from genetic changes, such as copy number gain and transcriptional activation in breast cancer [5]. We have previously shown that STAT3-induced IKBKE transcription and resulted in chemotherapy resistance in lung cancers [9]. It was also shown that

Address all correspondence to: Mokenge P. Malafa, MD, Department of Gastrointestinal Oncology, H. Lee Moffitt Cancer Center and Research Institute, 12902 Magnolia Drive, Tampa, FL, 33612, USA. E-mail: mokenge.malafa@moffitt.org

☆ **Funding**: This work was supported by funding from the NIH/NCI (RO1 to MPM and R01CA160455-01A to JQC). This work was also supported by the Moffitt Cancer Center Foundation. The H. Lee Moffitt Cancer Center and Research Institute is supported in part by NCI Cancer Center Support Grant P30 CA076292.
Received 8 August 2019; Revised 12 November 2019; Accepted 18 November 2019

1936-5233/19
https://doi.org/10.1016/j.tranon.2019.11.009

KRAS-induced IL-1β could upregulate IKBKE levels in nonsmall cell lung cancer cells and that these cells were sensitive to inhibition of IKBKE/TANK-binding kinase 1 (TBK1) [10]. Another study identified IKBKE as an important transcriptional target of Gli1 and a mediator of oncogenic activity of Gli1 in PDACs [11]. Moreover, upregulation of IKBKE induced cell transformation, cell survival, proliferation, migration/invasion, and chemoresistance, whereas depletion of IKBKE exerted opposite effects [5–9,11–14]. Although it belongs to the IκB kinase family, IKBKE only shares ~27% homology with IκB kinase-α and IκB kinase-β and 64% with TBK1. IKBKE activates nuclear factor-κB through phosphorylation of IκB-Ser32, CYLD-Ser418, TRAF2-Ser11, and p65-Ser536 [14–17], which leads to the induction of CCL5 and IL-6 and subsequent activation of the JAK/STAT3 pathway [10,18]. Our group previously showed that IKBKE directly phosphorylates AKT at Ser473 and Thr308, leading to AKT activation independent of phosphoinositide 3-kinase (PI3K) and mTORC2 complex [13]. IKBKE was shown to be upregulated in ~30% of breast cancer cases [5]. We have also shown that IKBKE is upregulated in ~50% of pancreatic cancer cases and that increased IKBKE expression is associated with poor patient survival [12]. Collectively, these studies show that IKBKE plays a pivotal role in human malignancy and could be a critical therapeutic target for PDAC.

Recent studies have identified two small-molecule compounds, amlexanox and CYT387, which directly inhibit IKBKE/TBK1 kinase activity [10,18,19]. Amlexanox is FDA approved for the treatment of aphthous ulcers and has been shown to reduce obesity in mice on high-fat diets by sensitizing cells to insulin [19]. CYT387 is a known JAK1/JAK2 inhibitor that is in clinical trials for myeloproliferative disorders [20–22]. CYT387 was also shown to inhibit IKBKE/TBK1 by direct inhibition of its kinase activity [10,18].

In this article, our aim was to investigate whether depletion of IKBKE reduced cell viability and CSC properties in PDAC. We also tested IKBKE inhibitors in vivo on tumor growth and metastasis of PDAC cells and in vitro in a mouse model. We studied the consequences of IKBKE inhibition on the receptor tyrosine kinase (RTK)/mitogen-activated protein kinase (MAPK) pathway. Finally, we combined IKBKE inhibitors with trametinib, an FDA-approved MEK inhibitor, to investigate the effects of this combination on PDAC growth and metastasis.

Materials and Methods

Cell lines and reagents

The PDAC cells were purchased from the American Type Culture Collection and used within 6 months of thawing. L3.6 pl, Mia Paca-2, and Panc1 PDAC cells were maintained in Dulbecco's Modified Eagle Medium (DMEM) (Gibco) with 10% FBS and 1% penicillin-streptomycin. ASPC1, T3M4, and BXPC3 PDAC cells were cultured in RPMI 1640 containing 10% FBS and 1% penicillin-streptomycin. HPNE-vec and HPNE-KRAS PDAC cells were cultured in media containing 75% DMEM with reduced glucose, 25% medium M3 base (Incell Corp, #M300F-500), 5% FBS, 10 ng/mL of recombinant human epidermal growth factor, and 750 ng/mL of puromycin. Amlexanox was purchased from Abcam, and CYT387 and trametinib were purchased from Selleckchem. For the in vivo studies, CYT387 and trametinib were purchased from APExBIO. The short hairpin RNAs (shRNAs) and expression plasmids for IKBKE have been previously described [6,7]. siRNAs for ErbB3 (Mission siRNA: SASI_Hs01_00196190) and IGF-1R (Mission siRNA: SASI_Hs01_00126194) were purchased from Sigma. Cell transfection was performed using Lipofectamine 2000 (Life Technologies), according to the manufacturer's protocol. All antibodies except IKBKE (Sigma), IGF-1R (Santa Cruz), Ki-67 (Abcam), and CD31 (Abcam) were purchased from Cell Signaling Technologies.

Cell viability and drug synergy studies

For cell viability, cells were plated at a density of 4000 cells/well in 96-well plates with quadruple wells for each treatment. siRNA transfections were performed 24 h after cells were plated. Inhibitor treatments were performed as indicated in the figure legends (Figures 1, 2 and 5 and Supplementary Figures 1 and 5). Cell viability was measured 72 h after treatment with thiazolyl blue tetrazolium bromide (MTT) (Sigma) according to the manufacturer's protocol.

For drug synergy studies, cells were treated with increasing concentrations (at equal ratios) of the inhibitors, and cell viability was measured as described previously [23]. Combination indices for each treatment were calculated using the Chou-Talalay method in CompuSyn [24].

Colonogenic survival (anchorage independent) growth assay

Standard soft agar colony formation assays were performed in Mia PaCa-2 and metastatic L3.6 pl cells. The treated cells were seeded at a density of 2000 per well in a 12-well plate in 0.3% agar over a 0.6% bottom agar layer. Colonies were fed with growth media and growth of colony formation was observed for 10 days. Colonies were photographed after overnight incubation with 1 mg/mL MTT in the wells. The colonies were counted under stereomicroscope and compared with control vehicle. Each experiment was performed in triplicate.

Migration and invasion assays

Cell migration and invasion assays were performed as described previously [25]. Indicated amounts of inhibitors were added to the top chamber, and the cells were allowed to migrate or invade at 37 °C for 16 h.

Three-dimensional matrigel spheroid culture

Cells were cultured in a three-dimensional on-top format as described previously [26], with slight modifications. Reduced growth factor Matrigel (2.5%, Corning) was used as the extracellular matrix, and cells were cultured for 4 days. Three-dimensional spheroids were counted using an inverted microscope at × 10 magnification.

Cancer stem cell assays

Cancer stem cell populations were determined using Aldefluor kit from Stemcell Technologies according to the manufacturer's protocol. Sphere assays were performed by growing cells at a density of 5 000 cells/well in ultralow attachment 6-well plates as described previously [27].

RNA isolation and reverse transcription-quantitative polymerase chain reaction

RNA was isolated using Trizol reagent from Life Technologies according to the manufacturer's instruction. Reverse transcription--quantitative polymerase chain reaction (PCR) was performed as described previously [25]. Primer sequences were as follows: for

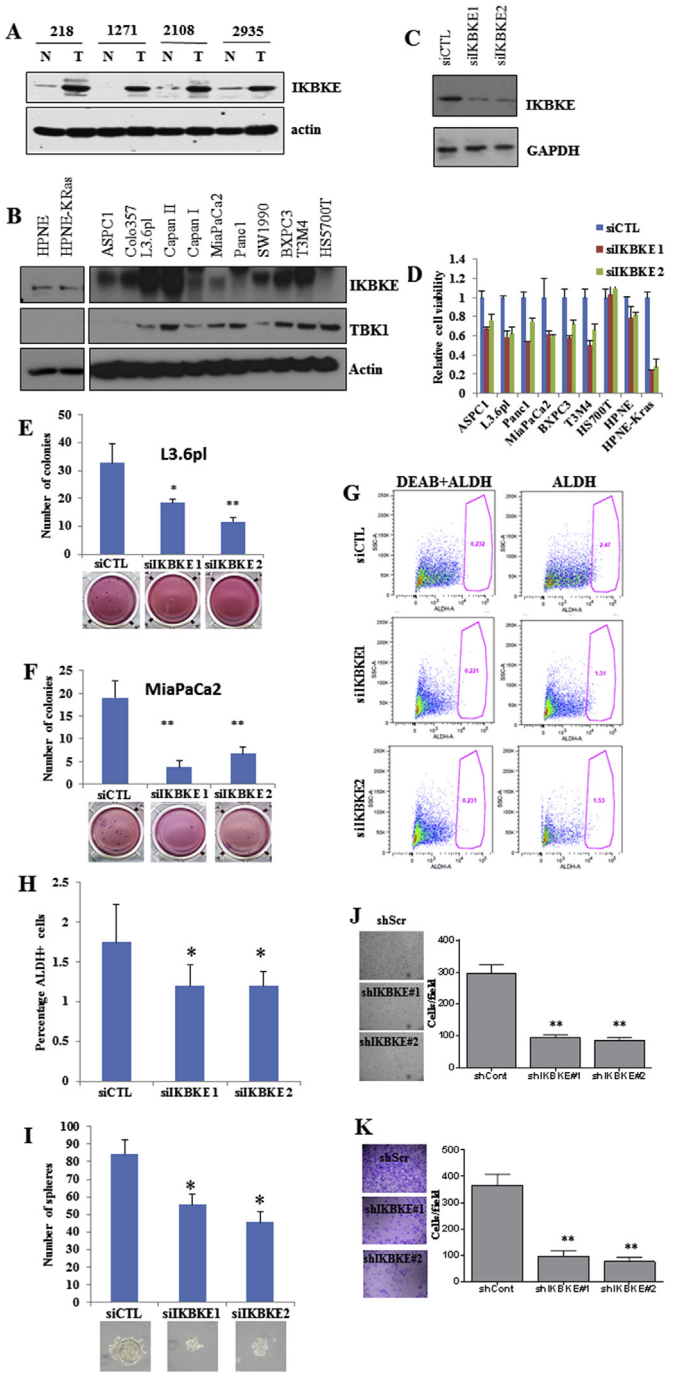

Figure 1. IKBKE is an important oncogene in pancreatic ductal adenocarcinoma. A, Lysates from human pancreatic tumor (T) and normal pancreas (N) and **B,** mutant KRAS or wild type KRAS PDAC cells were subjected to Western blot analyses with IKBKE and actin. **C and D,** PDAC cell lines were transfected with 2 siRNAs for IKBKE. MTT assay was performed 72 h after transfection. Knockdown efficiency of the siRNAs is shown. **E and F,** Soft agar colony formation assays in MiaPaCa-2 and metastatic L3.6 pl cells transfected with 2 siRNAs for IKBKE. Colonies were counted after 10 days. IKBKE knockdown significantly inhibited the colony formation. **G**–**H,** Aldefluor assays were performed on L3.6 pl cells with IKBKE knockdown or control cells as described in Materials and Methods. Diethylaminobenzaldehyde (DEAB) was used as a control. IKBKE knockdown significantly reduced the number of cancer stem cells. **I,** CSC spheres from control or IKBKE siRNA-transfected L3.6 pl cells. IKBKE knockdown significantly inhibited the sphere formation. **J**–**K,** L3.6 pl cells transfected with control siRNA or IKBKE siRNAs were plated in Boyden chambers for migration (**J**) or invasion (**K**) assays. *$P < .05$ and **$P < .002$.

ErbB3, forward 5′-ACAGTCTGCTGACTCCTGTT-3′ and reverse 5′-GAACTGAGACCCACTGAAGA-3’; for IGF-1R, forward 5′-TGTGTGGACCGTGACTTCTG-3′ and reverse 5′-GGACCTTCACAAGGGATGCA-3’ (IDT Technologies, Coralville, IA).

Phospho-RTK arrays

Phospho-RTK arrays (R&D Biosystems) were used as described previously [28], with slight modifications. The RTK membranes were incubated with 50 μg of lysates from L3.6 pl cells treated with 2 μM of CYT387 or vehicle for 24 h or 250 μg of lysates from L3.6 pl cells treated with 2 μM of CYT387 or vehicle for 36 h. Detection of activated RTKs was performed according to the manufacturer's protocol.

Animals and treatment

Female athymic nude mice (6 weeks old, 20−23 g) were purchased from Charles River (Wilmington, MA, USA). Mice (n = 20) were orthotopically implanted with luciferase-expressing L3.6 pl cells (1 million in 50 μL) to the pancreas. After 1 week, the mice were randomly divided into treatment and control groups. The mice were treated with vehicle or amlexanox at 50 mg/kg for 5 days/week. For CYT387 treatments, the mice were divided into 4 groups as follows: vehicle, CYT387, trametinib, and CYT387 plus trametinib. The mice were treated as described previously [18], at 10 mg/kg of CYT387 or 2.5 mg/kg of trametinib for 5 days/week. Drug treatments were performed by oral gavage. The tumor volume was measured once per week using IVIS 200 (Xenogen). After 4 weeks of treatment, the animals were killed and tumor weight and liver metastases were recorded. Half of the tumor tissues were immediately immersed in liquid nitrogen for biochemical analyses, and the remaining half were fixed in buffered formalin for histological analyses. The care and use of animals were approved by our Institutional Laboratory Animal Care and Use Committee and as per the guidelines of the National Institutes of Health.

Statistical analyses

One-way analysis of variance (ANOVA) was used for analyzing the animal experiments, and a two-tail unpaired *t*-test was used for analyzing statistics for all experiments performed.

Results

IKBKE knockdown led to decreased PDAC cell viability, CSCs, and invasion

We previously observed that IKBKE expression is elevated in approximately 50% of PDAC patients [12] and that higher levels of IKBKE correlate with poor patient survival. Moreover, we found that IKBKE expression is higher in early stages of pancreatic cancer, which is suggestive of its role in tumor initiation [12]. Here, we further showed that IKBKE expression is elevated in human pancreatic tumor compared with normal pancreas (Figure 1A) and in several PDAC cell lines (Figure 1B). To study the dependence of PDAC growth on IKBKE expression, we depleted IKBKE in a panel of PDAC cells

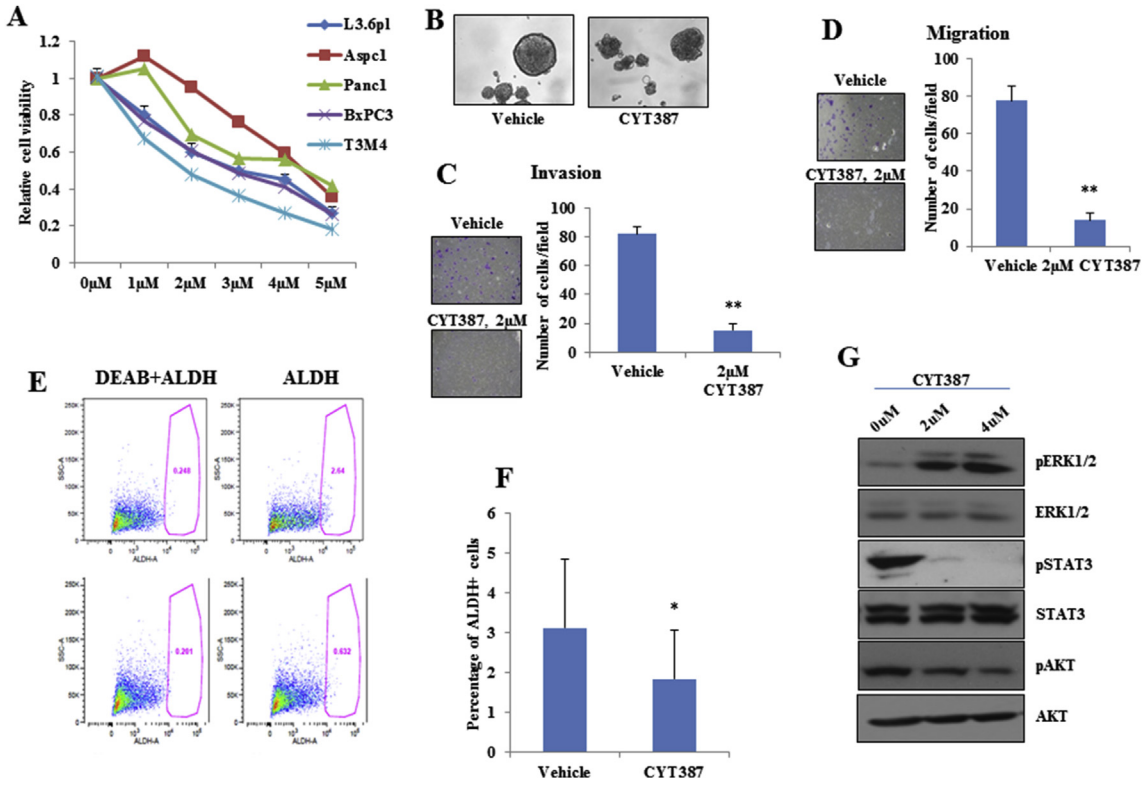

Figure 2. IKBKE/TBK1 inhibitor CYT387 reduced cell viability, cell motility, and cancer stem cell populations in PDAC cells. **A,** PDAC cell lines were treated with increasing concentrations of CYT387 and MTT assay was performed after 72 h. **B**, CYT387 inhibited L3.6 pl cell sphere formation compared with vehicle. **C and D,** L3.6 pl cells were plated with indicated amounts of CYT387 or vehicle for cell invasion (**C**) or migration (**D**) assays. **E and F,** L3.6 pl cells were treated with 2 μM of CYT387 for 96 h and ALDH-positive CSC population was assessed using Aldefluor kit. **G**, Western blot analyses of L3.6 pl cells treated with different doses of CYT387 for 24 h showed decreased phosphorylation of STAT3 and AKT and increased phosphorylation of ERK1/2. *$P < .05$ and **$P < .002$.

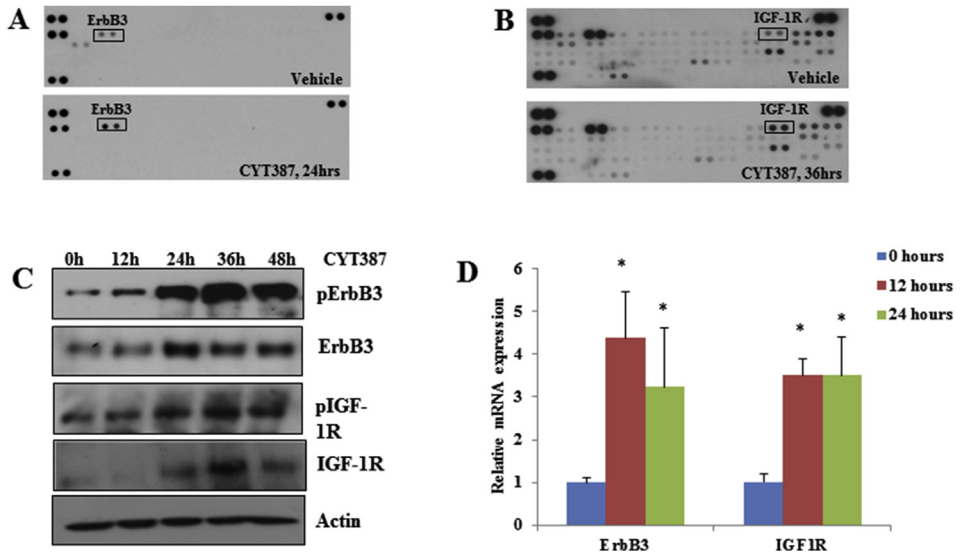

Figure 3. Inhibition of IKBKE leads to transcriptional upregulation of several RTKs. **A,** 50 μg of lysates from L3.6 pl cell treated with 2 μM of CYT387 for 24 h were incubated with phospho-RTK arrays. Western blot with pan-tyrosine antibody revealed activation of ErbB3. **B,** Phospho-RTK array analysis with 250 μg of lysates from L3.6 pl cells treated with 2 μM of CYT387 for 36 h showed significant activation of IGF-1R. **C,** Western blot analysis of lysates from L3.6 pl cells treated with 2 μM of CYT387 for indicated times showed increased activation and protein expression of IGF-1R and ErbB3. **D,** Quantitative PCR with ErbB3 and IGF-1R primers using RNA from L3.6 pl cells treated with 2 μM of CYT387 for indicated amount of time. Actin was used as a control. *$P < .05$.

using two different siRNAs and found that viability of these cells (anchorage-dependent and -independent growth) was lower when IKBKE was depleted (Figure 1C–F; Supplementary Figure 2). We noted that cells with wild type KRAS and low IKBKE were resistant to IKBKE knockdown. Because pancreatic CSCs are intrinsically resistant to many therapeutic agents, are highly tumorigenic, and are responsible for PDAC metastasis and treatment failure [4], we examined the effects of IKBKE on pancreatic CSCs. The population of pancreatic CSCs evaluated by aldehyde dehydrogenase (ALDH) staining was significantly lower in IKBKE siRNA-transfected cells compared with control siRNA (Figure 1G). Moreover, stem cell sphere growth was significantly reduced in IKBKE knockdown cells (Figure 1H). In addition, depletion of IKBKE led to decreased migration and invasion (Figure 1I and J) in L3.6 pl cells. These results demonstrate that IKBKE is important for PDAC cell survival and CSC growth and invasion.

Effect of pharmacological inhibition of IKBKE on PDAC phenotype

Amlexanox and CYT387 have recently been identified as inhibitors of IKBKE [10,19]. To study the efficacy of these inhibitors in PDAC, we treated 5 PDAC cell lines with increasing concentrations of amlexanox (Supplementary Figure 1A) and CYT387 (Figure 2A) and measured the cell viability using MTT assay. IC_{50} for growth inhibition of amlexanox and CYT387 were 50–100 μM and 2–4.5 μM, respectively. Interestingly, both inhibitors reduced three-dimensional sphere growth of L3.6 pl cells (Supplementary Figure 1B and Figure 2E). Consistent with the IKBKE knockdown data (Figure 1), inhibition of IKBKE with CYT387 reduced cell invasion (Figure 2C), migration (Figure 2D), and the percentage of ALDH-positive staining (Figure 2E and F) in L3.6 pl cells. Similar effects were observed when L3.6 pl cells were treated with amlexanox (Supplementary Figure 1C and 1D).

Amlexanox, an antiinflammatory agent, is an approved small-molecule therapeutic presently used in the clinic to treat aphthous ulcers and asthma [29,30] and is currently in clinical trial for obesity and type 2 diabetes [31]. To evaluate its antitumor activity in vivo, an orthotopic PDAC model was generated by injection of L3.6 pl cells into the pancreases of nude mice. After 1 week, the mice were randomly divided into 2 groups, one of which was orally treated with amlexanox and the other administered with vehicle. After the 4-week treatment, amlexanox led to modest reductions in tumor growth (Supplementary Figure 3A–C) and metastasis (Supplementary Figure 3D–F). Further investigation of xenograft tissues showed marked decreases in cell proliferation (Ki-67$^+$) and angiogenesis (CD31$^+$) (Supplementary Figure 3E). These data show that IKBKE inhibitors could have an antitumor effect in highly metastatic PDAC cells.

Inhibition of IKBKE leads to feedback activation of the RTKs/MAPK pathway by reactivation of FOXO3

To understand the effects of IKBKE inhibitors on downstream signaling, immunoblot analyses were performed in L3.6 pl cells treated with increasing concentrations of CYT387 (Figure 2G) or amlexanox (Supplementary Figure 4A) for 24 h. We found that both inhibitors abrogate phospho-AKT and phospho-STAT3, which are 2 major downstream targets of IKBKE [10,13]. We previously showed that IKBKE inhibition led to the activation of the ERK1/2 pathway [23] in nonsmall cell lung cancer cells. Therefore, we investigated whether IKBKE inhibitors induced ERK1/2 pathway in PDAC. Here, we found that IKBKE inhibition led to significantly increased pERK1/2 in multiple PDAC cell lines (Supplementary Figure 4B). Furthermore, immunostaining of amlexanox-treated orthotopic tumors also showed activation of ERK1/2 (Supplementary Figure 3E). A time course experiment in L3.6 pl cells showed prolonged activation of the BRaf-MEK-ERK pathway for up to 48 h after CYT387 treatment (Supplementary Figure 4C). To confirm that this feedback activation of ERK1/2 was because of IKBKE inhibition, we conducted Western blot analyses with lysates from IKBKE knockdown or control siRNA-treated L3.6 pl cells. IKBKE knockdown led to similar elevation of pERK1/2 (Supplementary Figure 4D).

It was previously shown that inhibition of AKT leads to feedback activation of RTK/MAPK by reactivation of FOXO3a, which induces RTK transcription [28]. Because IKBKE can inhibit FOXO3a by direct phosphorylation [7] or by activation of AKT, we hypothesized that inhibition of IKBKE-induced pERK1/2 could result from RTK activation. By hybridization of the phospho-RTK array with CYT387-treated and untreated cell lysates, we found that CYT387 treatment led to marked increases in phospho-ErbB3 and phospho-IGF-1R (Figure 3A and B). Time course studies with CYT387 showed that ErbB3 and IGF-1R activation was observed by 24 h. Furthermore, CYT387 treatment resulted in increased expression of ErbB3 and IGF-1R at protein (Figure 3C) and mRNA levels (Figure 3D).

We next examined whether ErbB3 and IGF-1R are required for IKBKE inhibition-mediated feedback of ERK1/2 activation. We transfected L3.6 pl cells with siRNAs of ErbB3 and IGF-1R followed by CYT387 treatment and found that knockdown of ErbB3 or IGF-1R significantly decreased CYT387-activated ERK1/2 (Figure 4A). Interestingly, we found that CYT387 inhibited phosphorylation of FOXO3a but induced total FOXO3a, ErbB3, and IGF-1R expression (Figure 4B). Knockdown of FOXO3 largely reduced CYT387-induced expression of ErbB3 and IGF-1R at protein and mRNA levels as well as pERK1/2 (Figure 4B and C). These results indicate that pharmacological and genetic inhibition of IKBKE feedback activates the MAPK pathway through induction of RTKs by reactivation of FOXO3.

Combination of IKBKE and MEK inhibitors inhibited PDAC cell survival, CSC renewal, tumor growth, and liver metastasis in an orthotopic PDAC model

Because inhibition of IKBKE feedback activates the MAPK pathway, we next investigated the effects of the combination of IKBKE and MEK inhibitors on PDAC cell viability, proliferation, and CSC growth. With the exception of ASPC1 cells, CYT387 synergized strongly with trametinib, an FDA-approved MEK inhibitor, in the PDAC cell lines tested (Figure 5A, Supplementary Figure 5). Furthermore, the combined treatment resulted in less colony growth than either agent alone (Figure 5B) and caused a dramatic decrease in CSC self-renewal (Figure 5C). Western blot analyses revealed that trametinib completely abrogated CYT387-induced ERK activation (Supplementary Figure 6A and B). In agreement with a previous report [32], we found that trametinib treatment alone induced pSTAT3, which was inhibited by the CYT387 treatment (Supplementary Figure 6A and B). Notably, the combined treatment led to a significant increase in Poly (ADP-ribose) polymerase cleavage (Supplementary Figure 6A).

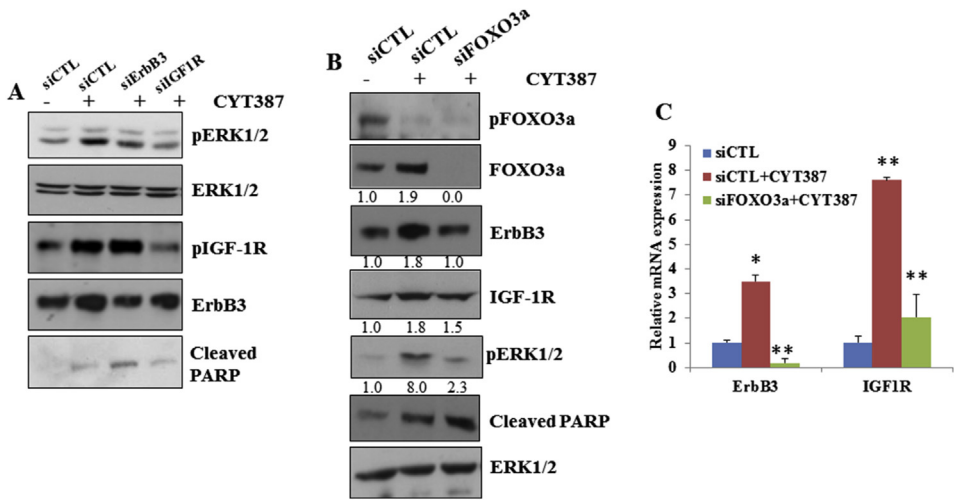

Figure 4. Inhibition of ErbB3 or IGF-1R inhibits CYT387-mediated ERK1/2 activation. **A,** 24 h after L3.6 pl cells were transfected with control siRNA or siRNAs targeting ErBB3 or IGF-1R, cells were treated with 2 μM of CYT387 for an additional 24 h and Western blot was performed using indicated antibodies. **B,** 36 h, h after L3.6 pl cells were transfected with control or FOXO3a-specific siRNAs, cells were treated with CYT387 for an additional 24 h and Western blot was performed using indicated antibodies. Band intensities were quantified using ImageJ software. **C,** L3.6 pl cells were treated as described in **B** and RNA was isolated. Quantitative PCR with ErbB3 and IGF-1R primers were performed. *$P < .05$ and **$P < .002$. Knockdown of FOXO3 reduced CYT387-induced expression of ERB3 and IGFR-1R miRNA levels.

We further tested the in vivo efficacy of IKBKE and MEK inhibitors alone and in combination in an orthotopic PDAC model. Tumor growth in our L3.6 pl cell-implanted mouse model was monitored weekly by Xenogen. Treatment with CYT387 alone showed a 37% decrease, trametinib resulted in a 45% decrease, and the combined treatment resulted in a 67% decrease in tumor volume (Figure 5D) as well as decreased tumor weight (Figure 5E). After 4 weeks of treatment, liver metastases were examined by Xenogen analyses of the removed livers and measured (Figure 5F). Liver metastasis was significantly lower in mice that received combined treatment than in mice treated with either CYT387 or trametinib alone (Figure 5F). Similarly, immunohistochemistry analyses showed an increase in apoptosis and a decrease in proliferating cells and angiogenesis with the combination treatment (Supplementary Figure 6C). Consistent with in vitro observations, CYT387 induced activation of ERK1/2 in vivo (Supplementary Figure 6B). Further analysis of the xenograft tissues by Western blot revealed that trametinib treatment led to a significant increase in phospho-AKT and the combination treatment abrogated these feedback activation events (Supplementary Figure 6B). Interestingly, Reverse transcription-quantitative PCR analyses showed that ErbB3 and IGF-1R expression levels were increased with CYT387 or trametinib treatment alone or in combination (Supplementary Figure 6D), supporting our findings and a previous report that inhibition of ERK1/2 led to increased ErbB3 and IGF-1R expression [33]. Together, these data indicate cotargeting IKBKE and its feedback activation pathway as a promising targeted therapy in PDAC.

Discussion

Although *KRAS* mutations are observed in about 95% of PDAC patients, targeting *KRAS* has not been successful. Therefore, it is important to understand and target the pathways downstream of *KRAS* signaling. In this study, we demonstrated that depletion of IKBKE reduces cell viability, CSC renewal, and cell motility in PDACs. Mutant *KRAS* was previously shown to regulate IKBKE expression through Gli transcription factor, and IKBKE expression correlated with poor survival in pancreatic cancer patients [11]. However, the efficacy of pharmacologic inhibitors of IKBKE was not evaluated in PDACs. In this study, we characterized IKBKE as a targetable pathway in PDAC. We also showed that amlexanox, a specific inhibitor of IKBKE/TBK1 that is in clinical trial for type 2 diabetes and obesity, and CYT387, a JAK and IKBKE/TBK1 inhibitor that is in clinical trials for myelodysplastic syndromes, are efficient in inhibiting cell viability, invasion, migration, and CSC population in vitro. These inhibitors showed moderate effects on tumor growth and metastasis in vivo, and we found that inhibition of IKBKE led to feedback activation of ERK1/2 because of rapid upregulation of ErbB3 and IGF-1R expression. We also report that the feedback activation of ErbB3/IGF-1R with CYT387 treatment is mediated by the release of suppression of FOXO3a, a known downstream target of IKBKE. This is the first report demonstrating preclinical evidence that IKBKE inhibitors are effective in PDAC. In addition, we provide mechanistic evidence for the feedback circuit that is activated after IKBKE inhibition.

MAPK and PI3K/AKT are major signaling cascades that mediate *KRAS* oncogenic activity [34], and combined inhibition of both the MAPK and PI3K/AKT pathways are currently being evaluated [35]. Here, we showed that IKBKE regulates multiple oncogenic pathways, such as AKT and STAT3 in PDAC. In addition, because inhibition of MAPK signaling leads to feedback activation of AKT [33] and STAT3 pathways [32], cotargeting IKBKE and MAPK signaling will be important in PDAC. Moreover, STAT3 pathway activation was shown to be responsible for increased metastasis of melanoma cells with MEK inhibition [32] and was implicated in resistance to several targeted therapies [36]. Hence, targeting IKBKE in these scenarios may show better efficacy. Similar to our results, ErbB3 and IGF-1R upregulation was implicated in therapeutic resistance in several studies [27,28,33,36–41], and we provide evidence that FOXO3a is required for this upregulation of RTKs.

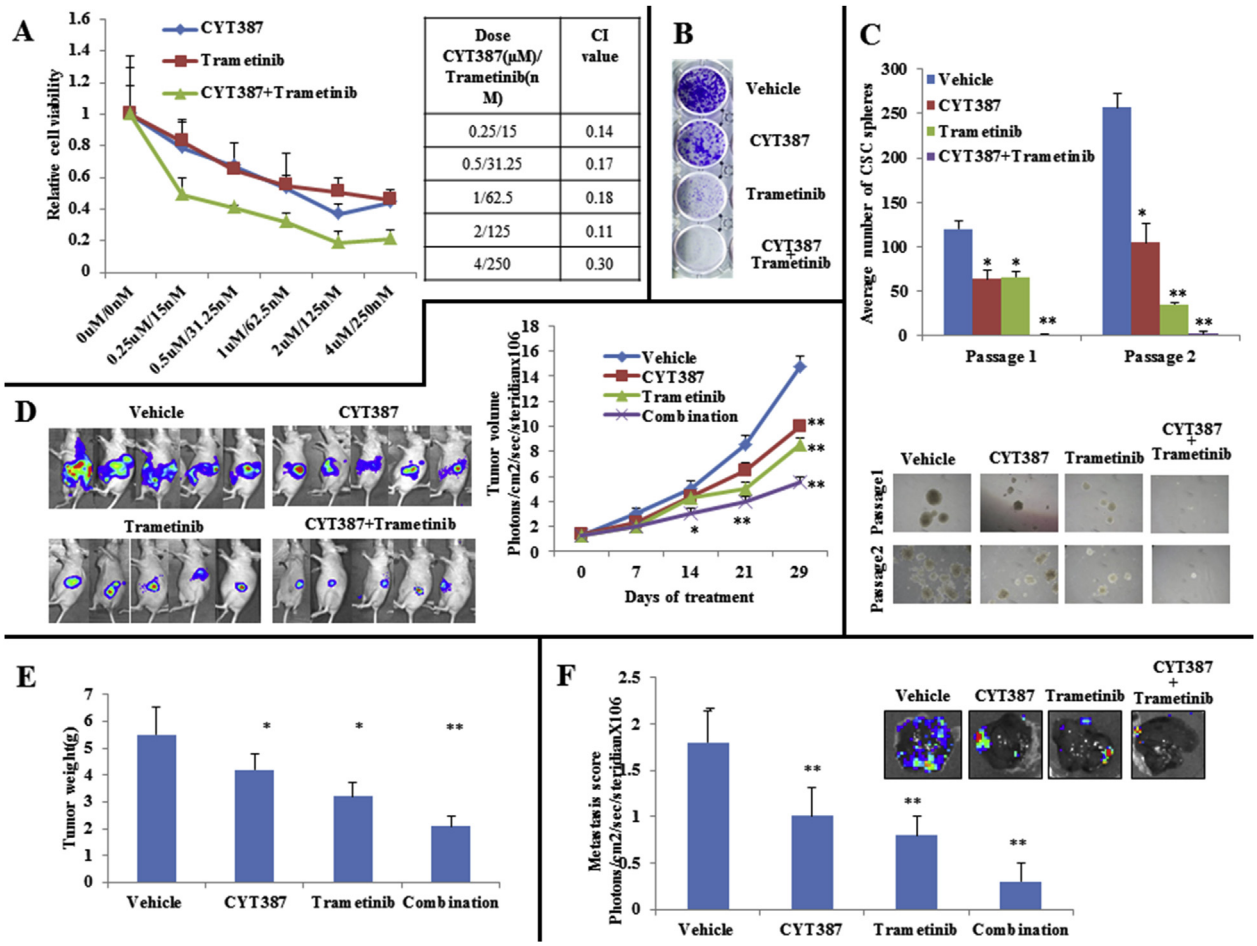

Figure 5. CYT387 synergizes with trametinib in pancreatic cells in vitro and in vivo. A, An MTT assay was performed on L3.6 pl cells that were treated with indicated amounts of CYT387 and trametinib for 72 h. CYT387 and trametinib show synergy in reducing cell viability. Combination indices are shown. **B,** L3.6 pl cells were cultured in 1 μM of CYT387 and 15 nM of trametinib or the combination for 10 days, and colonies were visualized by crystal violet staining. **C,** L3.6 pl cells were cultured under CSC culture conditions with 2 μM of CYT387 and/or 30 nM of trametinib. After 10 days, the number of spheres was counted. Two passages of cells were performed, with representative colony sizes shown. **D,** Tumor volumes of the L3.6 pl orthotopic tumors were measured once per week for 4 weeks. **E,** Tumor weights from mice bearing L3.6 pl orthotopic tumors and representative images of tumors at endpoint are shown. **F,** Liver metastasis scores at the endpoint. *$P < .05$ and **$P < .002$.

CSCs have been shown to be important for pancreatic tumorigenesis and metastasis [4,42]. In addition, stem cell–like cells have an ability to differentiate into endothelial cells and promote angiogenesis [43,44]. Interestingly, we found that IKBKE expression can modulate the CSC population. Although the mechanism by which IKBKE regulates CSCs is unknown, it was shown that TBK1, a homolog of IKBKE, plays a role in CSC self-renewal and tyrosine kinase inhibitor resistance in lung cancers [45]. Hence, inhibitors targeting IKBKE/TBK1 can potentially be used to reduce CSCs in PDAC.

Finally, we have shown that the IKBKE inhibitors synergize with the MEK inhibitor trametinib to reduce cell viability and CSC population in vitro and tumor growth and metastasis in vivo. We have also shown that the combination treatment synergistically reduced in vivo cell proliferation and angiogenesis. Of note, trametinib treatment in vivo led to an increase in phospho-AKT as shown before [33]. Hence, cotreatment with IKBKE inhibitors can increase the efficacy of trametinib. A phase I study is currently ongoing to identify the limiting dose of this combination in KRAS-mutant lung cancer patients who are resistant to platinum-based therapies (NCT02258607). Our results provide a strong rationale for similar trials in PDAC.

Limitations

It is important to note the limitations of our research. Firstly, the reason for the IKBKE band showing heterogeneity in Figure 1B is unknown; we suspect heterogeneity is because of the fact that different cell lines were used in the processing of IKBKE. Secondly, we do not know whether the decrease in IKBKE levels is because of knockdown or decreased viability in Figure 1D. We believe that knockdown occurred in Figure 1D on the basis of the results shown in Figure 1C. We acknowledge that a decrease in cell viability may not be because of the knockdown, but the likelihood is small. Thirdly, because of the nature of this type of biological research, it is difficult to definitively know if the <50% decrease in ALDH + indicates biological significance. A thorough discussion and further experimentation to identify whether the decrease is biologically significant is beyond the scope of this manuscript.

Declarations of interest

None.

Acknowledgments

The authors thank Paul Fletcher and Daley Drucker (H. Lee Moffitt Cancer Center and Research Institution) for editorial assistance. They were not compensated beyond their regular salary. The authors acknowledge the Small Animal Imaging Core, Flow Cytometry Core, and Molecular Genomics Core at H. Lee Moffitt Cancer Center and Research Institution.

Appendix A. Supplementary data

Supplementary data to this article can be found online at https://doi.org/10.1016/j.tranon.2019.11.009.

References

[1] Rahib L, Smith BD, Aizenberg R, Rosenzweig AB, Fleshman JM and Matrisian LM (2014). Projecting cancer incidence and deaths to 2030: the unexpected burden of thyroid, liver, and pancreas cancers in the United States. *Cancer Res* **74**(11), 2913–2921.

[2] Siegel RL, Miller KD and Jemal A (2018). Cancer statistics. *CA A Cancer J Clin* **68**(1), 7–30. 2018.

[3] Bryant KL, Mancias JD, Kimmelman AC and Der CJ (2014). KRAS: feeding pancreatic cancer proliferation. *Trends Biochem Sci* **39**(2), 91–100.

[4] Hermann PC, Huber SL and Herrler T, et al (2007). Distinct populations of cancer stem cells determine tumor growth and metastatic activity in human pancreatic cancer. *Cell stem cell* **1**(3), 313–323.

[5] Boehm JS, Zhao JJ and Yao J, et al (2007). Integrative genomic approaches identify IKBKE as a breast cancer oncogene. *Cell* **129**(6), 1065–1079.

[6] Guo JP, Shu SK and He L, et al (2009). Deregulation of IKBKE is associated with tumor progression, poor prognosis, and cisplatin resistance in ovarian cancer. *Am J Pathol* **175**(1), 324–333.

[7] Guo JP, Tian W, Shu S, Xin Y, Shou C and Cheng JQ (2013). IKBKE phosphorylation and inhibition of FOXO3a: a mechanism of IKBKE oncogenic function. *PLoS One* **8**(5):e63636.

[8] Hsu S, Kim M and Hernandez L, et al (2012). IKK-epsilon coordinates invasion and metastasis of ovarian cancer. *Cancer Res* **72**(21), 5494–5504.

[9] Guo J, Kim D and Gao J, et al (2013). IKBKE is induced by STAT3 and tobacco carcinogen and determines chemosensitivity in non-small cell lung cancer. *Oncogene* **32**(2), 151–159.

[10] Zhu Z, Aref AR and Cohoon TJ, et al (2014). Inhibition of KRAS-driven tumorigenicity by interruption of an autocrine cytokine circuit. *Cancer Discov* **4**(4), 452–465.

[11] Rajurkar M, De Jesus-Monge WE and Driscoll DR, et al (2012). The activity of Gli transcription factors is essential for Kras-induced pancreatic tumorigenesis. In: Proceedings of the national academy of sciences of the United States of America, vol. 109; 2012. E1038–E1047.

[12] Cheng A, Guo J, Henderson-Jackson E, Kim D, Malafa M and Coppola D (2011). IkappaB Kinase epsilon expression in pancreatic ductal adenocarcinoma. *Am J Clin Pathol* **136**(1), 60–66.

[13] Guo JP, Coppola D and Cheng JQ (2011). IKBKE protein activates Akt independent of phosphatidylinositol 3-kinase/PDK1/mTORC2 and the pleckstrin homology domain to sustain malignant transformation. *J Biol Chem* **286**(43), 37389–37398.

[14] Shen RR, Zhou AY, Kim E, Lim E, Habelhah H and Hahn WC (2012). IkappaB kinase epsilon phosphorylates TRAF2 to promote mammary epithelial cell transformation. *Mol Cell Biol* **32**(23), 4756–4768.

[15] Adli M and Baldwin AS (2006). IKK-i/IKKepsilon controls constitutive, cancer cell-associated NF-kappaB activity via regulation of Ser-536 p65/RelA phosphorylation. *J Biol Chem* **281**(37), 26976–26984.

[16] Hutti JE, Shen RR and Abbott DW, et al (2009). Phosphorylation of the tumor suppressor CYLD by the breast cancer oncogene IKKepsilon promotes cell transformation. *Mol Cell* **34**(4), 461–472.

[17] Shimada T, Kawai T and Takeda K, et al (1999). IKK-i, a novel lipopolysaccharide-inducible kinase that is related to IkappaB kinases. *Int Immunol* **11**(8), 1357–1362.

[18] Barbie TU, Alexe G and Aref AR, et al (2014). Targeting an IKBKE cytokine network impairs triple-negative breast cancer growth. *J Clin Investig* **124**(12), 5411–5423.

[19] Reilly SM, Chiang SH and Decker SJ, et al (2013). An inhibitor of the protein kinases TBK1 and IKK-varepsilon improves obesity-related metabolic dysfunctions in mice. *Nat Med* **19**(3), 313–321.

[20] Monaghan KA, Khong T, Burns CJ and Spencer A (2011). The novel JAK inhibitor CYT387 suppresses multiple signalling pathways, prevents proliferation and induces apoptosis in phenotypically diverse myeloma cells. *Leukemia* **25**(12), 1891–1899.

[21] Pardanani A, Laborde RR and Lasho TL, et al (2013). Safety and efficacy of CYT387, a JAK1 and JAK2 inhibitor, in myelofibrosis. *Leukemia* **27**(6), 1322–1327.

[22] Tyner JW, Bumm TG and Deininger J, et al (2010). CYT387, a novel JAK2 inhibitor, induces hematologic responses and normalizes inflammatory cytokines in murine myeloproliferative neoplasms. *Blood* **115**(25), 5232–5240.

[23] Challa S, Guo JP and Ding X, et al (2016). IKBKE is a substrate of EGFR and a therapeutic target in non-small cell lung cancer with activating mutations of EGFR. *Cancer Res* **76**(15), 4418–4429.

[24] Chou TC (2006). Theoretical basis, experimental design, and computerized simulation of synergism and antagonism in drug combination studies. *Pharmacol Rev* **58**(3), 621–681.

[25] Richards EJ, Zhang G and Li ZP, et al (2015). Long non-coding RNAs (LncRNA) regulated by transforming growth factor (TGF) beta: LncRNA-hit-mediated TGFbeta-induced epithelial to mesenchymal transition in mammary epithelia. *J Biol Chem* **290**(11), 6857–6867.

[26] Lee GY, Kenny PA, Lee EH and Bissell MJ (2007). Three-dimensional culture models of normal and malignant breast epithelial cells. *Nat Methods* **4**(4), 359–365.

[27] Matsubara S, Ding Q, Miyazaki Y, Kuwahata T, Tsukasa K and Takao S (2013). mTOR plays critical roles in pancreatic cancer stem cells through specific and stemness-related functions. *Sci Rep* **3**, 3230.

[28] Chandarlapaty S, Sawai A and Scaltriti M, et al (2011). AKT inhibition relieves feedback suppression of receptor tyrosine kinase expression and activity. *Cancer Cell* **19**(1), 58–71.

[29] Bell J (2005). Amlexanox for the treatment of recurrent aphthous ulcers. *Clin Drug Investig* **25**(9), 555–566.

[30] Makino H, Saijo T, Ashida Y, Kuriki H and Maki Y (1987). Mechanism of action of an antiallergic agent, amlexanox (AA-673), in inhibiting histamine release from mast cells. Acceleration of cAMP generation and inhibition of phosphodiesterase. *Int Arch Allergy Appl Immunol* **82**(1), 66–71.

[31] Reilly SM, Ahmadian M and Zamarron BF, et al (2015). A subcutaneous adipose tissue-liver signalling axis controls hepatic gluconeogenesis. *Nat Commun* **6**, 6047.

[32] Vultur A, Villanueva J and Krepler C, et al (2014). MEK inhibition affects STAT3 signaling and invasion in human melanoma cell lines. *Oncogene* **33**(14), 1850–1861.

[33] Turke AB, Song Y and Costa C, et al (2012). MEK inhibition leads to PI3K/AKT activation by relieving a negative feedback on ERBB receptors. *Cancer Res* **72**(13), 3228–3237.

[34] Pylayeva-Gupta Y, Grabocka E and Bar-Sagi D (2011). RAS oncogenes: weaving a tumorigenic web. *Nat Rev Cancer* **11**(11), 761–774.

[35] Engelman JA, Chen L and Tan X, et al (2008). Effective use of PI3K and MEK inhibitors to treat mutant Kras G12D and PIK3CA H1047R murine lung cancers. *Nat Med* **14**(12), 1351–1356.

[36] Lee HJ, Zhuang G, Cao Y, Du P, Kim HJ and Settleman J (2014). Drug resistance via feedback activation of Stat3 in oncogene-addicted cancer cells. *Cancer Cell* **26**(2), 207–221.

[37] Buck E, Eyzaguirre A and Rosenfeld-Franklin M, et al (2008). Feedback mechanisms promote cooperativity for small molecule inhibitors of epidermal and insulin-like growth factor receptors. *Cancer Res* **68**(20), 8322–8332.

[38] Chakrabarty A, Sanchez V, Kuba MG, Rinehart C and Arteaga CL (2012). Feedback upregulation of HER3 (ErbB3) expression and activity attenuates antitumor effect of PI3K inhibitors. In: Proceedings of the national academy of sciences of the United States of America, vol. 109; 2012. p. 2718–2723.

[39] Huang X, Gao L and Wang S, et al (2010). Heterotrimerization of the growth factor receptors erbB2, erbB3, and insulin-like growth factor-i receptor in breast cancer cells resistant to herceptin. *Cancer Res* **70**(3), 1204–1214.

[40] Montero-Conde C, Ruiz-Llorente S and Dominguez JM, et al (2013). Relief of feedback inhibition of HER3 transcription by RAF and MEK inhibitors attenuates their antitumor effects in BRAF-mutant thyroid carcinomas. *Cancer Discov* **3**(5), 520–533.

[41] O'Reilly KE, Rojo F and She QB, et al (2006). mTOR inhibition induces upstream receptor tyrosine kinase signaling and activates Akt. *Cancer Res* **66**(3), 1500–1508.

[42] Li C, Heidt DG and Dalerba P, et al (2007). Identification of pancreatic cancer stem cells. *Cancer Res* **67**(3), 1030–1037.

[43] Bao S, Wu Q and Sathornsumetee S, et al (2006). Stem cell-like glioma cells promote tumor angiogenesis through vascular endothelial growth factor. *Cancer Res* **66**(16), 7843–7848.

[44] Ricci-Vitiani L, Pallini R and Biffoni M, et al (2010). Tumour vascularization via endothelial differentiation of glioblastoma stem-like cells. *Nature* **468**(7325), 824–828.

[45] Seguin L, Kato S and Franovic A, et al (2014). An integrin beta(3)-KRAS-RalB complex drives tumour stemness and resistance to EGFR inhibition. *Nat Cell Biol* **16**(5), 457–468.